

Corrosion effects on tension stiffening behavior of reinforced concrete

M. A. Shayanfar[†] and M. Ghalehnovi[‡]

Civil Engineering Department, Iran University of Science and Technology, Narmak 16846, Tehran, Iran

A. Safiey^{‡†}

Civil Department, Moshanir Power Engineering Consultants, Park Prince Buildings, Vanak, Tehran, Iran

(Received January 10, 2007, Accepted August 26, 2007)

Abstract. The investigation of corrosion effects on the tensile behavior of reinforced concrete (RC) members is very important in region prone to high corrosion conditions. In this article, an experimental study concerning corrosion effects on tensile behavior of RC members is presented. For this purpose, a comprehensive experimental program including 58 cylindrical reinforced concrete specimens under various levels of corrosion is conducted. Some of the specimens (44) are located in large tub containing water and salt (5% salt solution); an electrical supplier has been utilized for the accelerated corrosion program. Afterwards, the tensile behavior of the specimens was studied by means of the direct tension tests. For each specimen, the tension stiffening curve is plotted, and their behavior at various load levels is investigated. Average crack spacing, loss of cross-section area due to corrosion, the concrete contribution to the tensile response for different strain levels, and maximum bond stress developed at each corrosion level are studied, and their appropriate relationships are proposed. The main parameters considered in this investigation are: degree of corrosion (C_w), reinforcement diameter (d), reinforcement ratio (ρ), clear concrete cover (c), ratio of clear concrete cover to rebar diameter (c/d), and ratio of rebar diameter to reinforcement percentage (d/ρ).

Keywords: reinforced concrete; tension stiffening; corrosion; average crack spacing; bond slip.

1. Introduction

Excessive tensile stresses result in cracking of a reinforced concrete member; as consequence of crack opening beyond a critical width, all of the applied tensile forces at the crack faces pass through the steel bars. Within two adjacent cracks, bond stresses between steel bar and surrounding concrete gradually transfer tensile forces from the steel reinforcement to the concrete; at the same time, these two materials slip on each other and develop the “tension stiffening” phenomenon. The tension stiffening is one of the essential elements of any reinforced concrete analytical model, in

[†] Associate Professor, Corresponding Author, E-mail: mohsenalishayanfar@gmail.com and shayanfar@iust.ac.ir

[‡] PhD Candidate

^{‡†} Engineer

particular in the analytical prediction of the response under service loads and the failure mode of a structure. To improve our knowledge about this phenomenon, the experimental studies are necessary to be undertaken; they are helpful to evade some difficulties observed in the analytical procedures. The results of the following experimental program could be used to develop a practical tension stiffening model for corroded and non-corroded reinforced concrete members (refer to Ghalehnovi, 2004 and Safiey, 2004).

Behavior of the reinforced concrete specimens in tension has been studied experimentally by numerous researchers such as: Goto (1971), Mirza and Houde (1979), Somoyaji and Shah (1981), Wollrab, *et al.* (1996), Cho, *et al.* (2004a), and Cho, *et al.* (2004b). These researchers provide valuable information about the tensile behavior of reinforced concrete members. But, it is necessary to accomplish these researches considering the effects of corrosion on tensile behavior of RC specimens.

Nowadays, one of the major concerns in serviceability of the reinforced concrete members in coastal regions is related to the destructive effects of the severe environmental conditions on steel bars resulting in gradual demolition of reinforced concrete structures. Severe damages are observed on almost all of the reinforced concrete structures which are located in the corrosive environments before termination of their expected service life. For instance, Palsson and Mirza (2002) planned a study for examining behavior of undamaged and corroded steel reinforcement from the abandoned deteriorated Dickson Bridge in Montreal, Canada. This case study gives an occurrence for demolition of an infrastructure due to exposing to the high corrosive environment.

Unfortunately, most of the available researches in this field were dedicated to study repair techniques and materials while few studies are devoted to develop analytical models for describing the behavior of corroded reinforced concrete members. However, there are some researchers, who tried to study and describe the behavior of corroded reinforced concrete members. The methodologies employed by the researchers in somehow are different from one to another; both experimental and analytical trends have been utilized. One of the most fundamental approaches to study the problem is adopting one of the standard tensile tests; this has to be conducted for the RC specimens with reinforcement corroded in different specific levels; refer to Amleh and Mirza (1999), Auyeung, *et al.* (2000), Behzadi Nejad Ahwazi, *et al.* (2001), and Fang, *et al.* (2004). In all of the above researches, the efforts were mainly concentrated on the deterioration of bond strength due to corrosion; but here, more attention had been paid to the "tension stiffening" of reinforced concrete members; the direct tension test was chosen for this purpose; this kind of tensile test is suitable for studying flexural bond between the steel bar and the concrete and the tensile cracks. The test set up is generally similar to those of Amleh and Mirza (1999) or Behzadi Nejad Ahwazi, *et al.* (2001). The study by Amleh and Mirza (1999) was mainly focused on the effects of different corrosion levels on bond strength of RC; while Behzadi Nejad Ahwazi, *et al.* (2001) went farther and studied the bond between steel and concrete using three different concrete mixes subjected to different corrosion levels. The current paper tries to illustrate the tensile behavior of reinforced concrete specimens and concentrates on evaluating the concrete stress contribution after cracking; the effects of corrosion on bond strength are also studied. It was planned to study the effects of some key parameters such as: degree of corrosion (C_w), reinforcement diameter (d), reinforcement ratio (ρ), clear concrete cover (c), ratio of concrete clear cover to rebar diameter (c/d), and ratio of rebar diameter to reinforcement ratio (d/ρ). Some empirical formulas to take into account corrosion effects on the tensile characteristics of reinforced concrete members were obtained by means of curve fitting techniques. The results of this study may be applicable for use to develop practical design codes or analytical reinforced concrete models used in nonlinear finite element analysis.

2. Experimental procedure

A total of 58 specimens have been prepared for the experimental program. Specimens were divided into 7 types according to their sizes (see Table 1). From each type, 2 specimens (totally 14) were used as control and were not placed in the corrosive conditions. The rest of the specimens (totally 44) have been kept in the corrosive environment until the expected level of corrosion achieved. Subsequently, all of the specimens including non-corroded samples were tested by direct tension test on the embedded rod.

2.1. Specimen design

Medium strength concrete (26 MPa) was used, and Type II cement. Sum of the water-cement and supplementary cementing materials ratios ($w/c+SCM$) was set to 52%; the weight of water, cement, sand and coarse aggregate in a volume unit of concrete admixture were 200, 385, 870, 885 kg/m³, respectively. The mean value of physical and mechanical properties of rebars and concrete were measured (Table 2). The compressive strength of the specimens was obtained by standard cylinder tests (100 mm diameter and 200mm height). The specimens were divided into seven types according to the rebar sizes and concrete covers, as cited on Table 1.

Concrete cylinder specimens had a constant 500 mm length and variable diameter ($D=60, 100, 150$ mm). One deformed steel reinforcement with 3 different diameter values ($d=12, 18, 25$ mm) has been embedded in the middle of the concrete cylinder. This steel bar was extended adequately outside the two ends of the specimen. The geometry of the specimen, schematically, is represented in Fig. 1. The specimen specifications are reported in Table 1. The specimen diameter (D) and reinforcement diameter (d) have been considered in a manner to facilitate the feasible study of the effects of some important parameters such as clear concrete cover (c), ratio of clear concrete cover to rebar diameter (c/d), and ratio of rebar diameter to reinforcement ratio (d/ρ). For the construction

Table 1 An overview on the specimens

Type	Specimen	c (mm)	ρ	c/d
1	S12-60	24	0.04	2.0
2	S12-100	44	0.0144	3.67
3	S18-60	21	0.09	1.167
4	S18-100	41	0.0324	2.278
5	S18-150	66	0.0144	3.67
6	S25-100	37.5	0.0625	1.5
7	S25-150	62.5	0.0278	2.5

Table 2 Material property of the specimens

Concrete			Reinforcement					
f'_t	E_c	f_c	$d = 12$ mm		$d = 18$ mm		$d = 25$ mm	
			E_s	f_y	E_s	f_y	E_s	f_y
1.62	24400	26	205000	515	200000	350	202000	369

Note: All properties are in MPa.

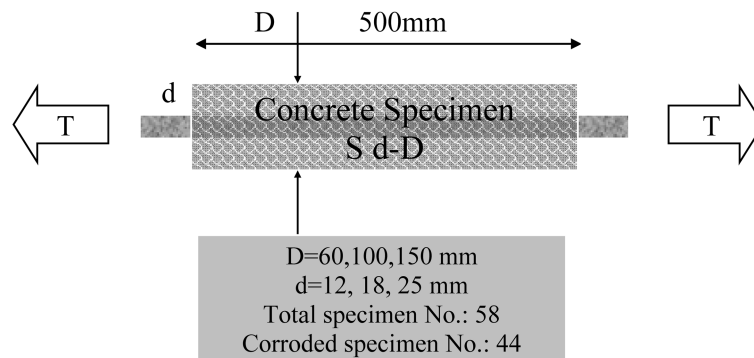


Fig. 1 Schematic representation of the geometry of reinforced concrete specimens

of the specimens, 500 mm long rubber molds have been used. The molds have been set on a special chassis, vertically. Steel reinforcement has been placed in the middle of the specimens to pass through the existing socket on an especial chassis at the end area. This set has been placed on a vibration table and the ready mixed concrete has been cast in mold layer by layer. After 24 hours, the molds have been opened and the specimens were cured at room temperature for 28 days.

2.2. Accelerated corrosion program

The exposed parts of the reinforcement and the end areas of the RC specimens at the top and bottom surface were coated by epoxy. The extended steel bar outside the concrete was covered by two layers of tape, electrical tape followed by duct tape. The specimens have been immersed into a fiberglass tub containing a solution of water and salt (5%). An electric supplier has been utilized to subject the specimens to voltage of 24 V and current density of 8 A. The direction of the electric current was set so that the reinforcement served as the anode while the bare metal wire which was spread over the specimens served as cathode (See Fig. 2). The duration of the accelerated corrosion procedure was estimated by Faraday's law to reach the required corrosion levels; with periods ranging



Fig. 2 Accelerated corrosion program

from one day to one month. The actual values of degree of corrosion were calculated by breaking the specimens to retrieve the reinforcing bar after completion of the tests. The reinforcement bar for each specimen was cleaned and carefully scrubbed with a wire brush to assure that the bar was free from any adhering corrosion products. Special attention had been paid not to alter the base metal. The reinforcing bar was then carefully weighed to determine the actual corrosion degree.

3. Experimental program

Details of the tensile test setup and instrumentation are presented in Fig. 3. Two special metal plates were fabricated, and each one was affixed to the top and the bottom of the specimens by three screws for measurement of specimen axial deformation. The LVDT (Linear Voltage Differential Transducer) system was employed to measure axial deformations. One gage was attached to the top plate and another one to the bottom plate for this purpose; the values of axial deformation of the specimen in each stage of loading were recorded by connecting them to the data logger apparatus. To measure reinforcing steel elongation, a displacement gage was affixed to the reinforcing bar at the top and another one at the bottom, connected to another LVDT system.

The axial tensile forces were applied by a hydraulic jack and measured by a load cell connected to the top bracket (refer to Fig. 3). The axial load values were measured continuously by a data logger equipment. The axial forces were increased to reach yielding capacity of the steel reinforcement; the tests were ceased by the onset of plastic deformations, and the number of

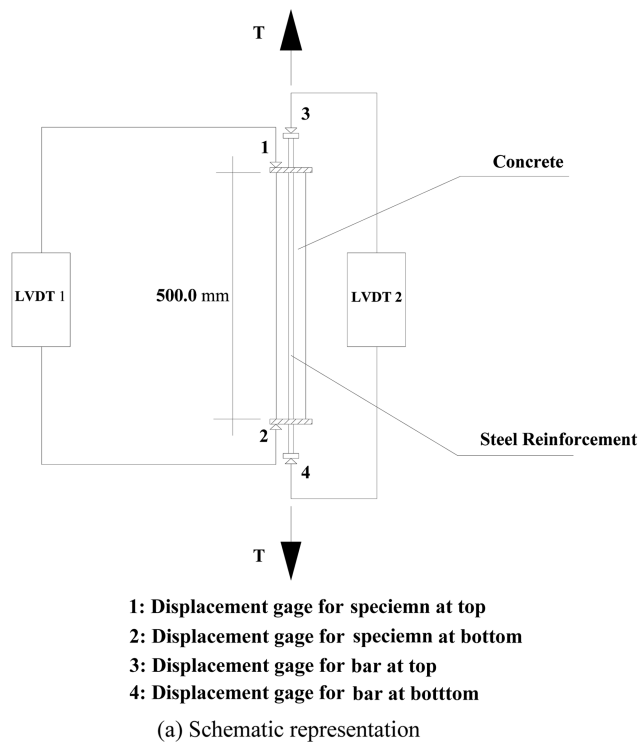


Fig. 3 Details of the direct tension tests



Fig. 4 Some of the direct tension tested specimens

transversal cracks and minimum and maximum crack spacing were recorded for each specimen. Photos of some of the specimens at the end of the tests are shown in Fig. 4. Eventually, actual degrees of the corrosion were measured for the corroded RC specimens as described earlier.

4. Experimental results and analysis

4.1. Corrosion levels

The expansion of the corrosion products cracks the concrete, longitudinally. Appearance of the first visible longitudinal crack was defined as the “first level of corrosion” and the corresponding degree of corrosion was denoted by C_{cr} ; before this corrosion level, the assumption of no bond deterioration between concrete and steel reinforcement is meaningful. There is a corrosion level before C_{cr} in which the bond strength of the specimen becomes maximum and greater than the one corresponding to undamaged specimen. This level of corrosion was denoted by C_0 .

The last important corrosion level is that in which no transversal crack (perpendicular to the steel reinforcement) is visible at the end of the direct tension test; this degree of the corrosion was named “ultimate corrosion level” (C_u); beyond this corrosion level, the bond between steel reinforcement and the surrounding concrete reaches its minimum value close to zero.

Regarding the above definitions and according to the experimental results (Table 3), it can be

Table 3 Important levels of corrosion (mass loss) of the specimens

Type of Specimen	c , mm	c/d	C_0 , %	C_{cr} , %	C_u , %
S12-60	24	2	0.9	2.8	10.0
S12-100	44	3.7	1.6	5.5	29.0
S18-60	21	1.2	0.5	1.5	10.0
S18-100	41	2.3	1.1	3.5	21.0
S18-150	66	3.7	1.8	7.0	32.0
S25-100	38	1.5	0.8	2.3	14.0
S25-150	63	2.5	1.3	4.0	22.0

concluded that:

Concrete specimen diameter or in other words concrete cover has a direct relationship with the “first level of corrosion” (C_{cr}), and the “ultimate corrosion level” (C_u).

The levels C_{cr} and C_u are inversely proportional to the steel bar diameter.

Consequently, the aforementioned corrosion levels could be proportional to the ratio c/d (c = clear concrete cover, d = steel bar diameter) according to the experimental results; these relationships were derived as follow by using least square curve fitting technique, (see Fig. 5):

$$C_{cr} = \frac{1.5c}{d}, \quad C_u = \frac{9c}{d} \quad (1)$$

The dispersion percentages of the measured first and ultimate corrosion levels in comparison to the predicted values by the above equations are 95.68 and 85.29, respectively.

4.2. Ultimate crack spacing

At the end of the direct tension tests, it was observed that the original specimens have been torn to several pieces with strongly variable lengths. It was clearly evident that the ultimate crack

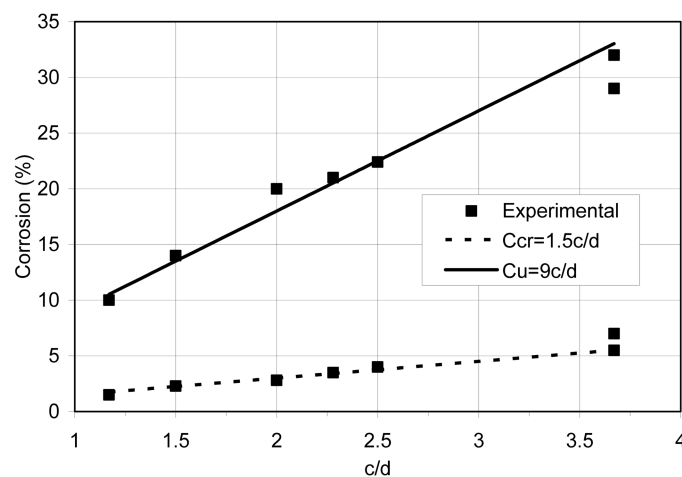


Fig. 5 Corrosion levels (Corrosion %=percentage of mass loss); a comparison between the experimental results and predictions of the proposed formulas

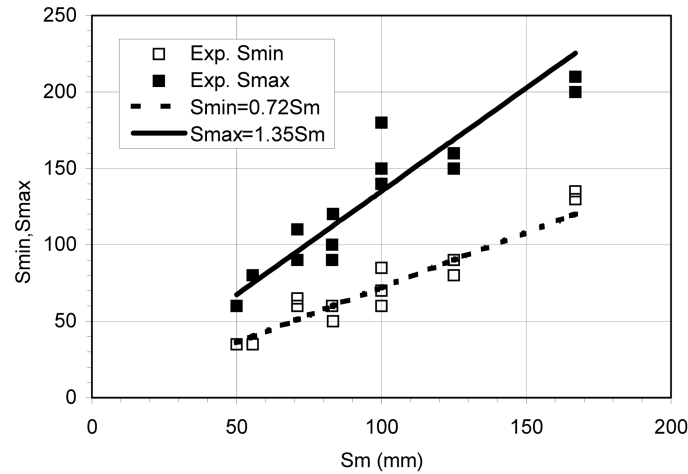


Fig. 6 Maximum and minimum crack spacing versus average crack spacing

spacing has a random nature. Ultimate maximum and minimum crack spacings were recorded for each specimen at end of the each direct tension test and accordingly, the average ultimate crack spacing was calculated ($S_m = 500 / (N_{cr} + 1)$). By means of the least square curve fitting technique applied to the experimental results (see Fig. 6), the ultimate average crack spacing, S_{m0} , for non-corroded specimens were related to the ultimate minimum and maximum crack spacing as below:

$$S_{\min} = 0.72S_{m0}, \quad S_{\max} = 1.35S_{m0} \quad (2)$$

The experimental results for non-corroded reinforced concrete specimens are available in Table 4; according to these results and by taking a look at the Table 1, these remarks could be explained regarding to S_{m0} :

(i) Concrete specimen diameter and reinforcing steel concrete cover have a direct relationship with the ultimate average crack spacing;

(ii) The ultimate average crack spacing has an inverse relationship with reinforcing steel diameter.

(iii) Increasing in the size (diameter) of the reinforcement bar and the concrete cover result in increasing the average crack spacing in the specimen.

These results agree well with established relations (CEB-FIB 1990, Rizkalla and Hwang 1984) showing that the average crack spacing, S_{m0} , could be expressed as a function of the rebar diameter, d , clear concrete cover, c , and ratios of c/d and d/ρ . By the means of the least square curve fitting techniques, these two formulas were proposed:

$$S_{m0} = 0.6(d + 40) + 0.21c + 0.009 \frac{d}{\rho} \quad (3)$$

$$S_{m0} = 2.35c \quad (4)$$

The comparison between predictions of these formulas with the ones proposed by Rizkalla and Hwang (1984) and CEB-FIB (1990) is illustrated in Fig. 7.

Another important factor which affects the ultimate crack spacing is the degree of the steel reinforcement corrosion. The proposed formulas for average crack spacing of non-corroded

Table 4 The results of the reinforced concrete specimens tests

Specimen	C_w (%)	N_{cr}	S_m (mm)	S_{min} (mm)	S_{max} (mm)	T_y (kN)	A_s (mm ²)	f_{bu} (MPa)	$A_{s,loss}$ (mm ²)
S12-60a	0.0	6	71.4	60.0	110.0	57.0	113.0	3.29	0.0
S12-60b	0.0	6	71.4	65.0	90.0	58.0	113.0	3.29	0.0
S12-60-1	2.8	6	71.4	50.0	97.0	55.0	107.0	3.29	5.04
S12-60-2	4.1	5	83.3	60.0	112.0	54.0	106.0	2.82	5.91
S12-60-3	10.5	3	125.0	90.0	170.0	49.0	97.0	1.88	14.6
S12-60-4	16.7	1	250.0	195.0	305.0	43.0	85.0	0.94	25.0
S12-60-5	20.0	0	500.0	-	-	40.0	79.0	0.47	29.9
S12-100a	0.0	4	100.0	70.0	180.0	59.0	113.0	6.65	0.0
S12-100b	0.0	4	100.0	85.0	150.0	58.0	113.0	6.65	0.0
S12-100-1	5.5	4	100.0	80.0	150.0	53.0	102.0	5.99	9.91
S12-100-2	9.0	3	125.0	90.0	170.0	48.0	93.0	5.32	17.9
S12-100-3	15.0	2	167.0	120.0	210.0	41.0	79.0	3.99	29.9
S12-100-4	22.0	1	250.0	180.0	320.0	33.0	64.0	2.66	43.2
S12-100-5	29.0	0	500.0	-	-	26.0	50.0	1.33	56.1
S18-60a	0.0	9	50.0	35.0	60.0	89.0	255.0	2.95	0.0
S18-60b	0.0	8	55.6	35.0	80.0	89.0	255.0	2.66	0.0
S18-60-1	1.0	8	55.6	40.0	75.0	89.0	255.0	2.66	0.0
S18-60-2	1.5	8	58.8	45.0	80.0	88.0	252.0	2.52	1.01
S18-60-3	3.0	6	71.4	50.0	100.0	88.0	250.0	2.07	1.69
S18-60-4	4.0	5	83.3	55.0	105.0	85.0	243.0	1.78	4.49
S18-60-5	6.5	3	125.0	85.0	150.0	83.0	238.0	1.18	6.63
S18-60-6	8.0	2	167.0	115.0	200.0	82.0	234.0	0.89	7.98
S18-60-7	9.0	1	250.0	190.0	310.0	81.0	232.0	0.59	8.99
S18-60-8	10.0	0	500.0	-	-	80.0	227.0	0.3	10.7
S18-100a	0.0	5	83.3	50.0	120.0	90.0	255.0	5.23	0.0
S18-100b	0.0	4	100.0	60.0	140.0	89.0	255.0	4.35	0.0
S18-100-1	1.1	5	83.3	60.0	115.0	89.0	252.0	5.27	1.01
S18-100-2	3.5	4	100.0	70.0	135.0	85.0	242.0	4.39	5.03
S18-100-3	7.0	3	125.0	90.0	165.0	80.0	227.0	3.51	10.9
S18-100-4	9.0	3	125.0	92.0	170.0	78.0	221.0	3.51	13.2
S18-100-5	11.5	2	167.0	110.0	210.0	73.0	209.0	2.63	18.0
S18-100-6	13.0	2	167.0	120.0	220.0	71.0	201.0	2.63	21.1
S18-100-7	16.0	1	250.0	170.0	330.0	66.0	188.0	1.76	26.3
S18-100-8	18.0	1	250.0	175.0	325.0	63.0	179.0	1.76	29.8
S18-100-9	21.0	0	500.0	-	-	57.0	163.0	0.88	36.0

specimen (Eqs. (3), (4)) shall be modified to account for the reinforcement corrosion degree. Fig. 8 shows the effects of corrosion on the ratio of S_m/S_{m0} (that is a ratio of ultimate crack spacing in corroded condition to the non-corroded condition for similar specimen). Figs. 8(a) and (b) show the

Table 4 The results of the reinforced concrete specimens tests (Continued)

Specimen	C_w (%)	N_{cr}	S_m (mm)	S_{min} (mm)	S_{max} (mm)	T_y (kN)	A_s (mm ²)	f_{bu} (MPa)	$A_{s,loss}$ (mm ²)
S18-150a	0.0	2	167.0	155.0	190.0	89.9	255.0	5.98	0.0
S18-150b	0.0	2	167.0	150.0	180.0	91.0	255.0	5.98	0.0
S18-150-1	1.8	3	143.0	110.0	185.0	86.0	244.0	6.98	4.0
S18-150-2	2.5	2	167.0	110.0	195.0	84.0	237.0	5.98	6.89
S18-150-3	5.0	2	167.0	105.0	230.0	79.0	224.0	5.98	12.0
S18-150-4	7.0	2	167.0	120.0	225.0	75.0	212.0	5.98	16.6
S18-150-5	12.0	2	200.0	135.0	235.0	66.0	187.0	4.98	26.7
S18-150-6	15.5	2	200.0	135.0	245.0	58.0	164.0	4.98	35.7
S18-150-7	20.0	1	250.0	200.0	300.0	53.0	149.0	3.99	41.6
S18-150-8	26.5	1	333.0	240.0	260.0	42.0	119.0	2.99	53.3
S18-150-9	32.0	0	500.0	-	-	32.0	90.0	1.99	64.6
<hr/>									
S25-100a	0.0	5	83.3	60.0	90.0	180.0	491.0	3.66	0.0
S25-100b	0.0	5	83.3	60.0	100.0	180.0	491.0	3.66	0.0
S25-100-1	2.3	5	90.9	66.0	125.0	173.0	471.0	3.35	4.0
S25-100-2	5.7	3	125.0	90.0	155.0	166.0	452.0	2.44	8.0
S25-100-3	11.2	1	250.0	190.0	310.0	155.0	422.0	1.22	14.0
S25-100-4	14.0	0	500.0	-	-	149.0	407.0	0.61	17.0
<hr/>									
S25-150a	0.0	3	125.0	80.0	150.0	181.0	491.0	5.67	0.0
S25-150b	0.0	3	125.0	90.0	160.0	182.0	491.0	5.67	0.0
S25-150-1	4.0	3	143.0	100.0	182.0	172.0	464.0	4.96	5.51
S25-150-2	9.4	2	167.0	120.0	205.0	153.0	412.0	4.25	16.0
S25-150-3	16.0	1	250.0	200.0	300.0	129.0	349.0	2.84	29.0
S25-150-4	22.4	0	500.0	-	-	105.0	285.0	1.42	42.0

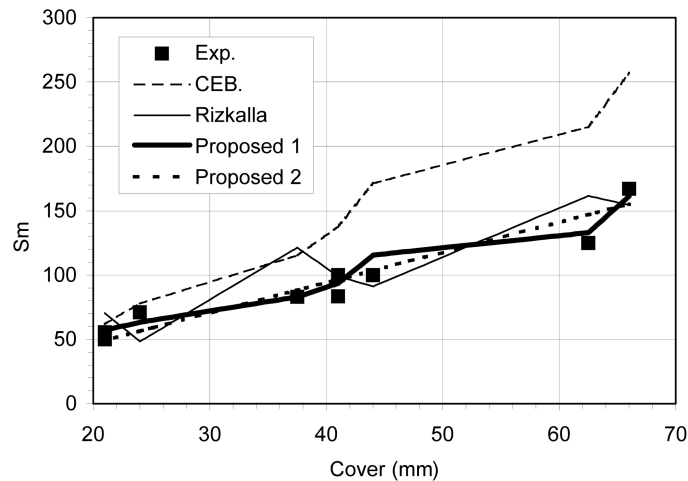


Fig. 7 Crack spacing, a view over the predictions of experimental data and analytical formulas

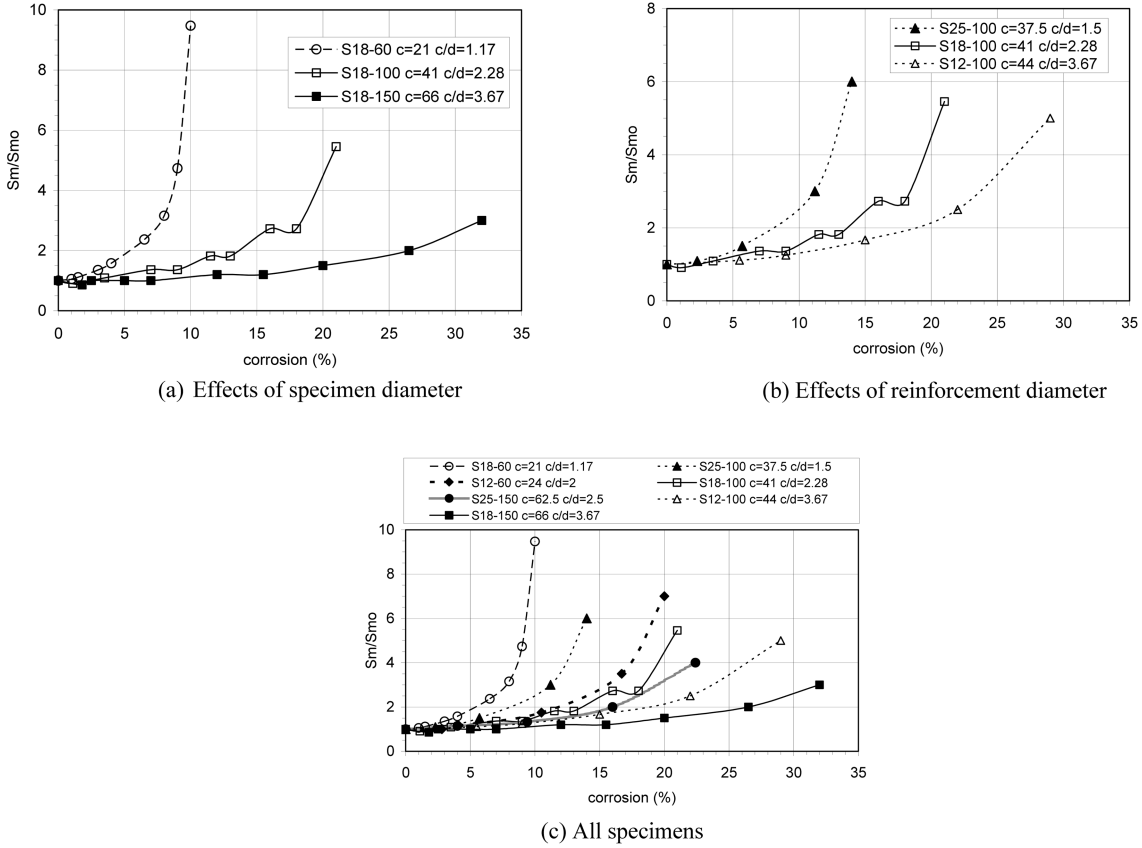


Fig. 8 Corrosion effects on the ultimate crack spacing

effects of the specimens diameter and the rebars diameter on the ratio of S_m/S_{m0} , respectively. As can be learnt from Fig. 8(a), for the specimens with equal reinforcement diameter ($d=18$ mm), the specimens diameter ($D=60, 100$ and 150 mm) has an inverse effect on the ultimate crack spacing ratio (S_m/S_{m0}). Also, it can be observed from Fig. 8(b), that for the specimens with equal diameters ($D=100$ mm), the rebar sizes ($d=12, 18$ and 25 mm) affect the S_m/S_{m0} ratio, directly. In Fig. 8(c), the S_m/S_{m0} ratios were plotted versus different corrosion levels for the 7 types of specimen. Considering these results, the following relation was obtained by the means of least square curve fitting technique (see Table 4):

$$\frac{S_m}{S_{m0}} = 1.533 - 0.3\frac{c}{d} + 4.2\left(\frac{C_w}{C_u}\right)^2 \tag{5}$$

In this equation, the parameter S_{m0} should be predicted by Eq. (3) or Eq. (4) and the ultimate corrosion level (C_u) could be estimated by Eq. (1). The dispersion percentage of the predicted values in comparison to the experimental results for Eq. (3) and Eq. (5) combination is equal to 96.6 and the dispersion percentage for Eq. (4) and Eq. (5) combination is equal to 96.33 for predicting the experimental results.

4.3. Concrete stress contribution

The concrete stress contribution in tension in post cracking state was studied to improve knowledge about the tension stiffening in the reinforced concrete members. To draw the plots of concrete stress contributions versus average steel reinforcement strain contributions, the following procedure was used.

Consider the equilibrium equation for a reinforced concrete specimen between steel reinforcement and the concrete as:

$$T = F_s + F_c \quad (6)$$

Since the steel reinforcement remains linear elastic to the end of the test, the reinforcement contribution of tensile force (F_s) could be computed by:

$$F_s = A_s \cdot E_s \cdot \varepsilon_{sm} \quad (7)$$

Substituting Eq. (7) into Eq. (6) and solving it for F_c , the concrete stress contribution could be calculated as:

$$\sigma_{cm} = \frac{F_c}{A_c} = \frac{T - A_s E_s \varepsilon_{sm}}{A_c} \quad (8)$$

The average steel reinforcement strain, ε_{sm} , and the corresponding total applied load, T , have been measured continuously during the tests for each specimen. Using Eq. (8) and the experimental data, the stress-strain curves of the specimens have been plotted as shown in Fig. 9. These curves represent the concrete stress contributions versus the average steel reinforcement strain contributions. These curves show that by increasing the degree of corrosion, the tension stiffening is affected in these manners: (i) the slope of the concrete stress contribution-average reinforcement strain curve becomes steeper, and (ii) the ultimate tensile strain reduces consequently. These alterations can be related to the loss of bond strength and reinforcement cross-section area due to the corrosion of steel rebars. Increase in the degree of corrosion reduces the bond strength in the similar specimens; therefore, the total applied loads transfer within a greater length from the steel reinforcement to the surrounding concrete and with larger deformations. It was also observed that for similar specimens, the degree of steel reinforcement corrosion has an inverse effect on the number of transversal cracks.

It can be learnt from Fig. 9 that by increasing the degree of steel reinforcement corrosion, the concrete stress contribution is reduced in post cracking state; for high degrees of corrosion, the concrete stress contribution is extremely reduced. Also, it was observed that after a specific average steel reinforcement strain, the concrete stress contribution reduces to the zero value. This strain limit was denoted by ε_{cw} and referred to as "ultimate tensile strain". By the means of the least square curve fitting technique, the following formula was obtained for estimation of this parameter:

$$\frac{\varepsilon_{cw}}{\varepsilon_y} = 0.907 - 0.757 \frac{C_w}{C_u} + 0.0087 \frac{C}{d} \quad (9)$$

For non corroded specimens, the concrete stress contribution drops to zero value when the average strain of the reinforcement reaches the yielding strain; but for corroded specimens, this

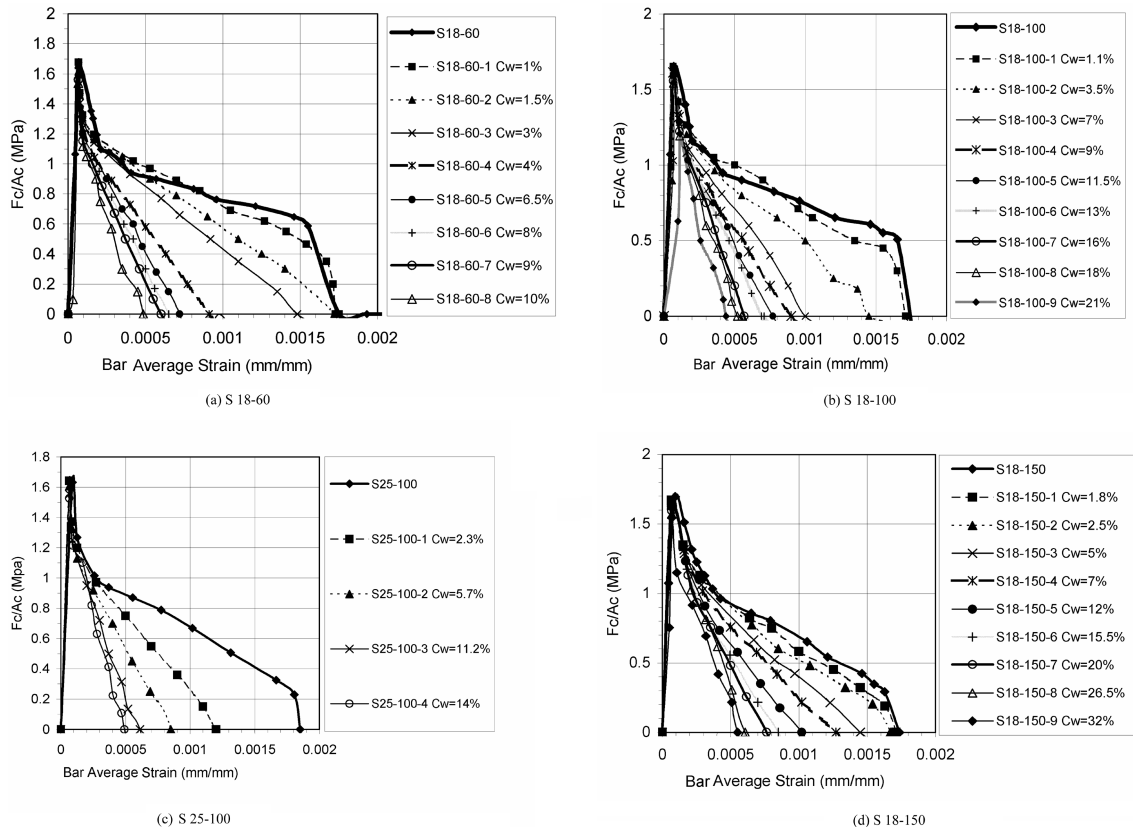


Fig. 9 Concrete stress contribution-steel reinforcement average strain curve of RC specimens

happens at a smaller steel reinforcement strain. Eq. (9) reveals that ultimate tensile strain could be affected not only by degree of reinforcement corrosion but also by the other parameters such as the concrete cover thickness and reinforcement diameter.

The tension-stiffening curve consists of three distinct phases. For non-corroded members, these three distinct states are: Non-cracking state, Multiple cracking state and Final cracking state (e.g. refer to Choi and Cheung 1996). As it was expected, the non-cracking state is not affected by the corrosion but the cracking states are significantly degraded by the extension of the corrosion degree. In the extensive corrosion condition, the multiple cracking state disappears, completely. Generally, it can be concluded that by increasing the degree of steel bar corrosion, the concrete tensile force contribution decreases.

4.4. Bond strength

In a reinforced concrete member after formation of the first tensile crack, by increasing the applied tensile loads, concrete cracks form and open progressively until the ultimate crack pattern is achieved. In the post cracking state, slip takes place between reinforcing steel and concrete. The values of the mean bond stresses are not constant in this state and increase with the slip, accordingly.

Consider concrete between two adjacent cracks as shown in Fig. 10(a). The average tension forces on the concrete and the resultant of reinforcement steel interface stresses are equal to $f_{bm}\pi da$. To develop a new crack in concrete, the concrete stress has to reach to its maximum value (f_t); equilibrium of the forces for concrete as shown in Fig. 10(b) results in:

$$f_{bm} = \frac{f_t A_c}{\pi da} \tag{10}$$

Showing that the average bond stress between concrete and steel has an inverse relationship with spacing between two adjacent cracks. The numbers of the tensile cracks remain constant by onset of reinforcement yielding at crack faces; thereafter, the value of the average bond stress reaches to its maximum value which is almost constant and equal to f_{bu} . At this stage, Eq. (10) can be rewritten in the following form (see Fig. 10(c)):

$$f_{bu} = \frac{2f_t \cdot A_c}{\pi d S_m} \tag{11}$$

The values of S_m for each test were computed (see Table 4). Mean ultimate bond stress of the specimens (f_{bu}) were computed and presented in Table 4.

As it could be observed from Table 1 and Table 4, c/d ratio plays a key role in the ultimate bond strength of the specimens. By utilizing least square curve fitting technique, the following formula was proposed:

$$f_{bu0} = 0.4 \frac{c}{d} \sqrt{f_c} (MPa) \tag{12}$$

In which, f_{bu0} is the ultimate bond stress without corrosion consideration. In Fig. 11, the predictions of the proposed formula were compared with the similar ones (Chan, *et al.* 1992, ACI 318-99, ABA-99) and experimental results.

The graphs of f_{bu}/f_{bu0} versus C_w (actual degree of corrosion) were plotted in Fig. 12(a) to (c) to show the effects of the different parameters. It can be observed that there is a little bond strength increase at first levels of corrosion. By formation of the first longitudinal crack (at the first level of

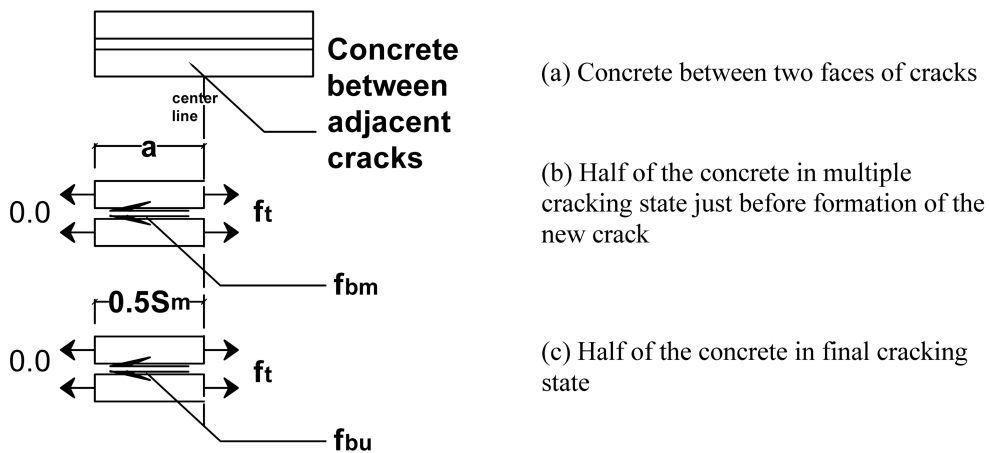
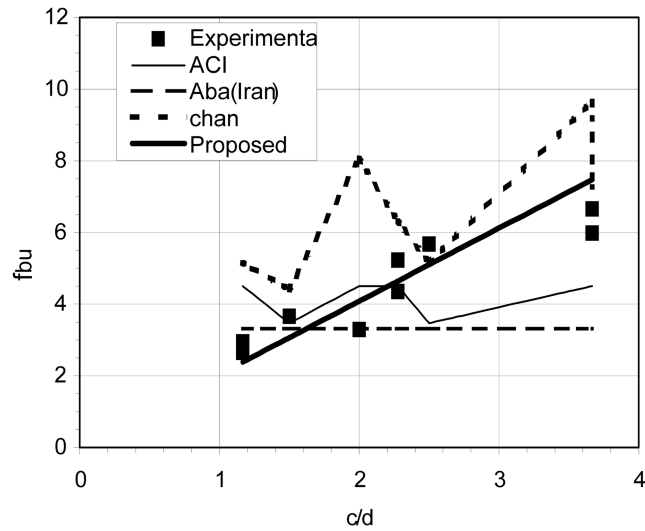
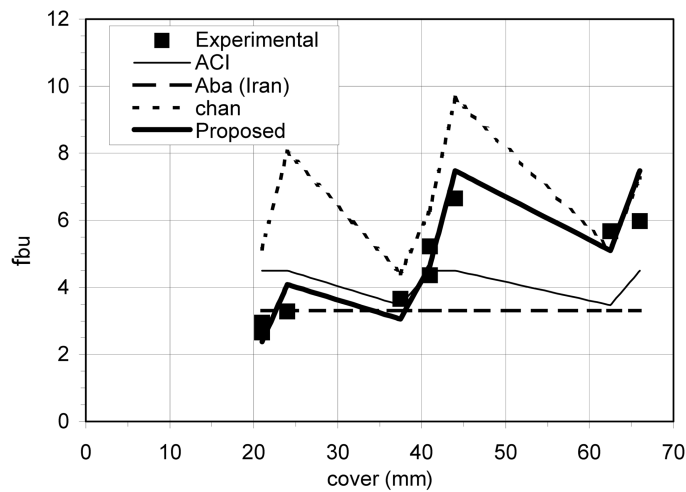


Fig. 10 Free body diagrams



(a) *c/d* ratio versus ultimate bond strength



(b) Concrete cover versus ultimate bond strength

Fig. 11 Comparisons between analytical and experimental ultimate bond strength

corrosion, C_{cr}), increasing corrosion levels decrease the ultimate bond strength.

Eq. (12) could be modified to include the corrosion effects. It can be learnt from Eq. (11) that the ultimate bond strength (f_{bu}) has an inverse relationship with ultimate average crack spacing; therefore, this relationship can be written for a specific specimen in corroded and non-corroded states:

$$\frac{f_{bu}}{f_{bu0}} = \frac{S_{m0}}{S_m} \tag{13}$$

In the above equation, subscript 0 means the non-corroded condition. Similar to the Eq. (5), the ratio of f_{bu}/f_{bu0} could be expressed as a function of the ratios of c/d and C_w/C_u . By means of the

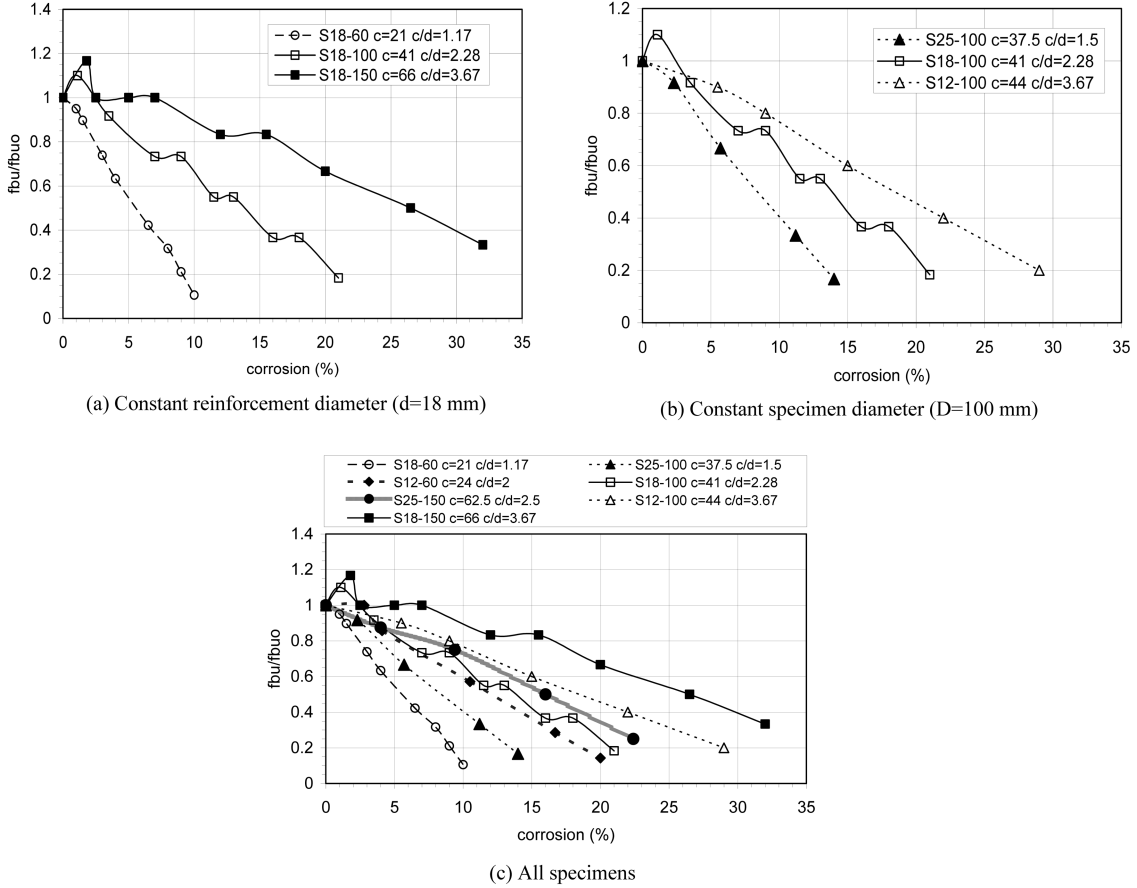


Fig. 12 Effects of degrees of corrosion (percentage of mass loss) on bond strength

curve fitting techniques, the following equation was suggested for calculating ultimate bond strength of a reinforced concrete member considering corrosion effects:

$$\frac{f_{bu}}{f_{bu0}} = 0.932 + 0.044 \frac{c}{d} - 0.823 \frac{C_w}{C_u} \tag{14}$$

In the above equation f_{bu0} is ultimate bond strength without considering corrosion effects which can be estimated by Eq. (12). The dispersion of the combination of Eq. (12) and Eq. (14) for predicting the experimental results are 96.89%. Amleh and Mirza (1999) did not propose any equation similar to Eq. (14) for prediction corrosion effects on ultimate bond strength; but, the total trends represented in Fig. 12 agrees well with their findings. Moreover, Stanish, *et al.* (1999) in an experimental research program proposed the following formula for the ultimate bond strength:

$$\frac{f_{bu}}{\sqrt{f_c}} = 0.63 - 0.041 C_w(\%) \tag{15}$$

Their experiments were designed in a manner to represent the anchorage bond. Therefore, Eq. (15) represents the corrosion effects on the ultimate anchorage bond strength; whereas, Eq. (12) and

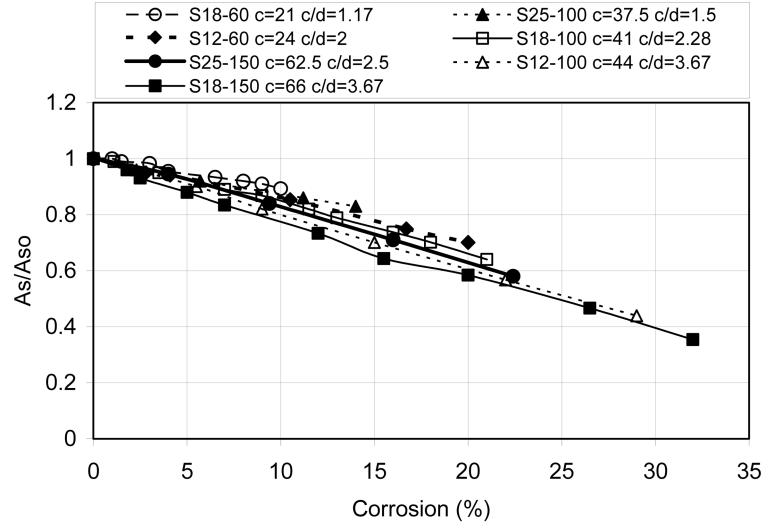


Fig. 13 Effects of degrees of corrosion (percentage of mass loss, %) on reinforcement cross section

(14) are derived upon the direct tension test; the setup of this kind of test is designed in a manner to study the flexural bond, not the anchorage bond. Moreover, some of the important factors (e.g. clear concrete cover) had been neglected in Stanish, *et al.* (1999) study. It can be learnt from Eq. (15) that whenever C_w exceeds a specific value ($15.37\% = 0.63/0.041$), the ultimate bond strength becomes zero; while some of the other parameters (mainly the ratio of concrete cover to the steel reinforcement diameter) control the ultimate degree of corrosion as shown earlier.

4.5. Effect of corrosion on the cross-section area of the reinforcement

In direct tension tests, the applied load was increased to reach the yielding limit of the reinforcing steel bar of the each specimen (T_y); at this stage, the test was stopped. Assuming that the yield stress of reinforcing rebar remains unchanged due to the corrosion effects as:

$$f_y = \frac{T_{y0}}{A_{s0}} = \frac{T_y}{A_s} \quad (16)$$

In the above relationship, the subscript 0 indicate the characteristics of the non-corroded condition. Since the values of T_y and T_{y0} are known; the ratio of A_s/A_{s0} can be computed easily. The computed values of A_s is represented in Table 4. The A_s/A_{s0} ratios versus different degrees of the corrosion are plotted in Fig. 13 for all types of the specimens. Because of non uniform distribution of corrosion over the reinforcement, an experimental relationship would be used to represent the equivalent cross-section area of a corroded steel rebar embedded in a specific concrete member. The following formula was proposed by the means of the least square curve fitting technique to the experimental results:

$$\frac{A_s}{A_{s0}} = 1.2 - 0.08 \frac{c}{d} - 0.35 \frac{C_w}{C_u} \quad (17)$$

The dispersion of this relationship against the experimental results is 98.4%.

4.6. Specimens' total applied tensile load versus average reinforcement strain

The total applied tensile force versus the average reinforcement strain curves (hereafter total strength curve) were plotted and studied for each specimen as illustrated in Fig. 14. These curves are useful for studying the corrosion effects on the concrete tensile force contribution. Fig. 14 represents the total strength (force) curves for four specimen types with different corrosion levels. It is evident from Fig. 14 that the slope of the total strength curves and yielding limit of specimens diminish by increasing the steel bar corrosion level. The loss of steel reinforcement cross-section area and deterioration of the bond between the steel reinforcement and concrete are the main sources for these changes. Deterioration of the bond decreases the concrete force contributions and results in the reduction of the total specimen stiffness leading to a decrease in the slope of the response.

It was observed from the experiments that the specimens with higher degrees of corrosion have a smaller number of cracks, while they posse larger deformations in comparison to the other specimens at multiple cracking state. In other words, larger deformations are necessary for development of the transversal cracks at increasing degrees of corrosion. Bond deterioration means the reinforcement transfers its force to the surrounding concrete within a greater length with larger deformation.

Investigation of these curves for the specimens with different concrete covers and identical rebar

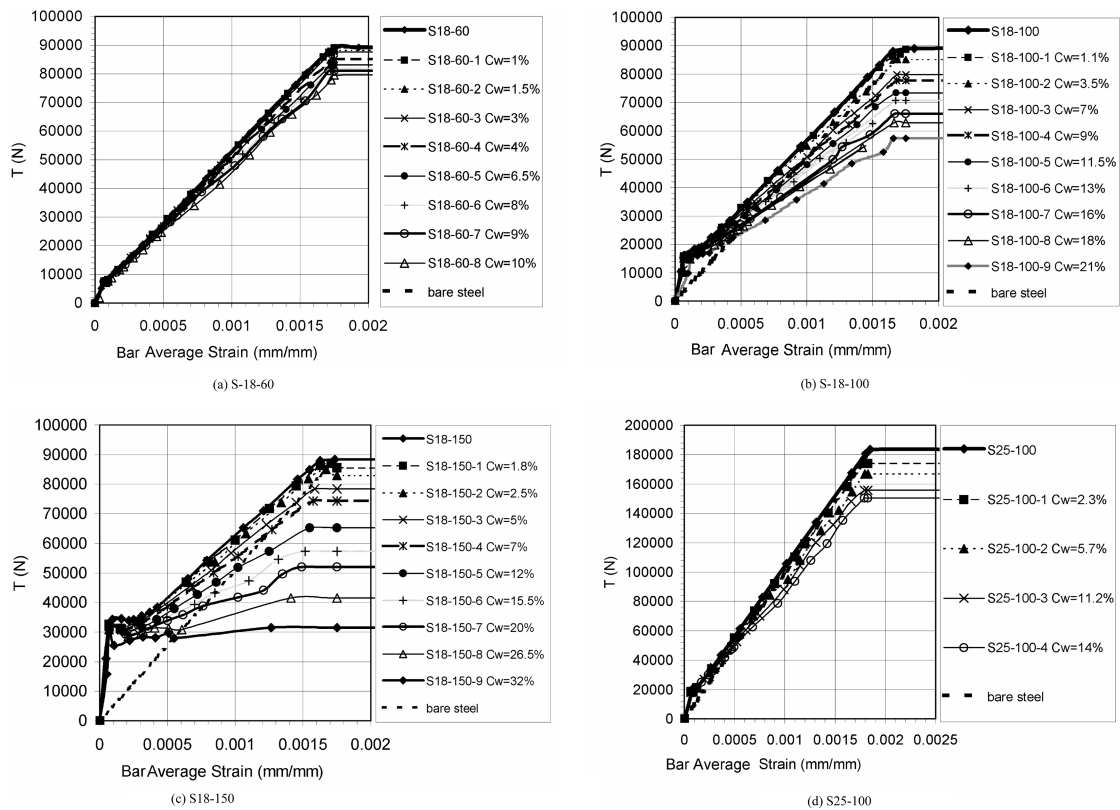


Fig. 14 Effects of degrees of corrosion on total applied load (T) versus reinforcement average strain

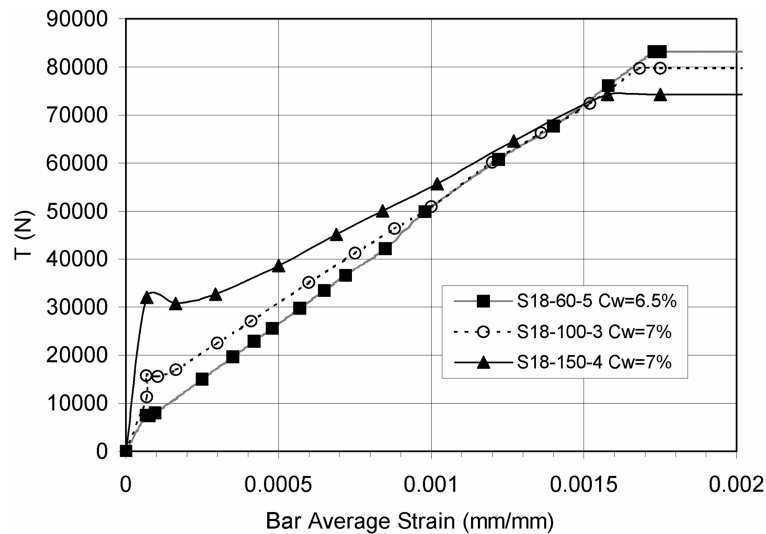


Fig. 15 Clear concrete cover effects on total applied load (T) versus reinforcement average strain for specimens with identical rebar diameters subjected to the similar degrees of corrosion

sizes subjected to the same degrees of the corrosion (Fig. 15) shows that the increase on cover, increases the total strength of the specimen until the ultimate limit state; thereafter, it behaves in the contrary. This behavior could be related to the more probable nonlocalized steel reinforcement corrosion in the specimen with thicker concrete cover.

5. Comparisons and validations

In this section, the validity of the proposed equations is verified; since these are obtained from curve fitting of the experimental results, it is important to verify them by comparing their predictions to the results of similar experiments. In this respect, the experimental program of Amleh

Table 5 Comparisons between predictions of the proposed formulas and experimental results from Amleh and Mirza (1999)

Specimen	C_w	S_m			f_{bu} / f_{bu0}		A_s / A_{s0}	
		Exp.	Ana. Eqs. (3), (5)	Ana. Eqs. (4), (5)	Exp.	Ana. Eq. (14)	Exp.	Ana. Eq. (17)
SS1,SS2	0.0	83.3	90.3	90.3	1.0	-	1.0	-
CS1	4.0	90.9	100.1	104.85	0.91	0.85	0.983	0.96
CS2	5.5	100.0	115.77	121.25	0.83	0.78	0.973	0.93
CS3	11.0	167.0	215.51	225.72	0.5	0.54	0.9	0.83
CS4	11.5	200.0	227.87	238.672	0.42	0.51	0.883	0.82
CS5	12.0	238.0	240.78	252.19	0.35	0.49	0.873	0.81
CS6	17.5	-	-	-	0.08	0.25	0.8	0.71

and Mirza (1999) was chosen, similar to that presented in this paper. The test specimens were cylindrical, 1 m long, 100 mm in diameter, and reinforced with a single bar with 19.5 mm nominal diameter. The corresponding comparisons are presented in Table 5. The results confirm the validation of the proposed empirical formulas.

6. Conclusions

The tensile behavior of reinforced concrete considering corrosion effects was studied experimentally. The specimen properties were chosen in a manner to reflect the effects of the governing parameters in the tensile behavior of the reinforced concrete specimens. The following conclusions are drawn:

(i) Two important corrosion levels (C_{cr} and C_u) have direct relationship with c/d . The former corresponds to the opening of the first longitudinal crack, and the latter to complete bond breakdown. Therefore, increasing the concrete cover and using finer reinforcement sizes will increase C_{cr} and C_u ; this rule of thumb would be applicable to improve the durability of a reinforced concrete member in a corrosive environment.

(ii) (a) The ultimate crack spacing for non-corroded specimens mainly is related to the clear concrete cover of specimens. (b) This length will be increased for corroded specimens by increasing the degree of corrosion and appearance of longitudinal cracks. (c) This is merely related to the decline of the bond between concrete and steel reinforcement demanding for greater length to transfer tensile forces from the steel to the concrete.

(iii) The study of the specimens concrete stress contribution versus steel reinforcement average strain reveals that the tension stiffening of reinforced concrete is very sensitive to the degree of reinforcement corrosion. Severe corrosion results in bond breakdown between concrete and steel reinforcement; nearby no contribution of the concrete in the tensile response beyond cracking (tension cut-off) could be expected for specimens in such condition. The lower levels of the reinforcement corrosion have considerable impacts on the stiffness and the ultimate strain of the tension stiffening curve. The ultimate tensile strain of these curves for non corroded specimens is close to the reinforcement yielding strain, but it will be reduced nearby to the strain corresponding to the tensile strength of concrete by increasing the levels of corrosion. The study on total applied tensile forces versus the average reinforcement strain curves also shows that the corrosion will decrease concrete stress contribution in cracking states.

(iv) The study of ultimate average bond strength deterioration of specimens and loss of cross-section area of reinforcement as result of corrosion reveals that the c/d ratio (the ratio of clear concrete cover to the size of the reinforcement) has an important role in controlling these two important effects of corrosion.

(v) Some empirical formulas for prediction of some of the studied parameters (e.g. ultimate crack spacing) were proposed and compared with the experimental findings of a similar program. Acceptable correlations were observed between the results of these two research programs.

Generally, the guidelines provided in this paper will be useful for development a tension stiffening model for the corroded reinforced concrete members to be used in conjunction with a nonlinear finite element formulation for reinforced concrete structures.

Appendix

The dispersion of the proposed relationships in comparison to experimental results presented throughout the article were obtained by the following formula:

$$Di = \left(1 - \frac{1}{N} \sqrt{\sum_{i=1}^N \left(\frac{X_{\text{exp},i} - X_{\text{pre},i}}{X_{\text{exp},i}} \right)^2} \right) \times 100 \quad (1)$$

In which, Di is dispersion percentage, $X_{\text{exp},i}$ is the experimental value, N denotes the total number of specimens, and $X_{\text{pre},i}$ represents the predicted value by the proposed formula.

Notation

- a = half of spacing between two subsequent cracks
- A_c = net concrete cross-section area
- A_s = reinforcement cross-section area
- A_{s0} = reinforcement cross-section area without considering corrosion effect
- c = clear concrete cover
- C_0 = corrosion level corresponding to the first bond strength increase
- C_{cr} = corrosion level corresponding to the first longitudinal crack
- C_u = ultimate corrosion level
- C_w = corrosion level
- d = reinforcement diameter
- D = specimen diameter
- E_c = concrete initial modulus of elasticity
- E_s = steel reinforcement initial modulus of elasticity
- f_{bm} = mean bond strength
- f_{bu} = ultimate bond strength
- f_{bu0} = ultimate bond strength without corrosion effect consideration
- f_c = concrete compressive strength
- f_t = concrete tensile strength
- f'_t = nominal concrete tensile strength
- f_y = yielding stress of the steel reinforcement
- F_c = concrete force contribution
- F_s = steel reinforcement force contribution
- N_{cr} = number of transversal cracks observed in each specimen at end of direct tension tests
- S_m = ultimate average crack spacing between two adjacent cracks
- S_{m0} = ultimate crack spacing between two adjacent cracks without considering corrosion
- S_{max} = ultimate maximum crack spacing between two adjacent cracks
- S_{min} = ultimate minimum crack spacing between two adjacent cracks
- T = applied tensile load
- T_y = applied tensile load corresponding to yield strength
- T_{y0} = applied tensile load corresponding to yield strength without considering corrosion

- ε_{sm} = reinforcement steel average strain
 ρ = reinforcement ratio
 σ_{cm} = concrete average stress

References

- ACI Committee 318 (1999), "Building code requirement for structural concrete and commentary", *ACI 318-99*, American Concrete Institute, Chicago.
- Amleh, L. and Mirza, M. S. (1999), "Corrosion influence on bond between steel and concrete", *ACI Struct. J.*, **96**(3), 415-423.
- Auyeung, Y. B., Balaguru, P. and Chung L. (2000), "Bond behavior of corroded reinforcement bars", *ACI Mater. J.*, **97**(2), 214-220.
- Behzadi Nejad Ahwazi, B., Amleh, L. and Mirza, M. S. (2001), "Effect of corrosion on bond strength of reinforcing bar in concrete", *Proceedings of First International Conference on Concrete & Development, Tehran, Iran*, 309-330.
- CEB-FIB (1990), "Model code for concrete structures", *Comite Euro International du Béton*, Paris, 437.
- Chan, H. C., Cheung, Y. K. and Huang, Y. P. (1992), "Crack analysis of reinforced tension member", *ASCE J. Str. Eng.*, **118**(8), 2118-2132.
- Cho, J. Y., Kim, N. S., Cho, N. S. and Choi, I. K. (2004a), "Cracking behavior of reinforced concrete panel subjected to biaxial tension", *ACI Struct. J.*, **101**(1), 76-84.
- Cho, J. Y., Kim, N. S., Cho, N. S. and Choun, Y. S. (2004b), "Stress-strain relationship of reinforced concrete subjected to biaxial tension", *ACI Struct. J.*, **101**(2), 202-208.
- Choi, C. K. and Cheung, S. H. (1996), "Tension stiffening model for planar reinforced concrete members", *Comput. Struct.*, **59**, 179-190.
- Fang, C., Lundgren, K., Chen, L. and Zhu, C. (2004), "Corrosion influences on bond in reinforced concrete", *Cement Concrete Res.*, **34**, 2159-2167.
- Ghalehnovi, M. (2004), "Characteristic relations in nonlinear finite element analysis with considering corrosion and bond-slip", PhD thesis, Iran University of Science and Technology, Tehran (In Persian).
- Goto, Y. (1971), "Cracks formed in concrete around deformed tension bars", *Proceedings ACI J.*, **68**(4), 244-281.
- Management and Programming Institute (1999), "Iranian concrete code (ABA)", Publication No. 120, Tehran, Iran (In Persian).
- Mirza, M. S. and Houde, J. (1979), "Study of bond stress slip relationships in reinforced concrete", *Proceedings ACI J.*, **76**(1), 19-45.
- Palsson, R. and Mirza, M. S. (2002), "Mechanical response of corroded steel reinforcement of abandoned concrete bridge", *ACI Struct. J.*, **99**(2), 157-162.
- Rizkalla, S. H. and Hwang, L. S. (1984), "Crack prediction for members in uniaxial tension", *Proceedings ACI J.*, **81**, 1984, 572-579.
- Safiey, A. (2004), "Nonlinear finite element analysis of RC beams and columns taking into account corrosion and bond-slip", MS thesis, Iran University of Science and Technology, Tehran (In Persian).
- Somoyaji, S., and Shah, S. P. (1981), "Bond stress versus slip relationships and cracking response of tension members", *ACI J.*, **78**, 217-225.
- Stanish, K., Hooton, R. D. and Pantazopoulou, S. J. (1996), "Corrosion effects on bond strength in reinforced concrete", *ACI Struct. J.*, **96**(6), 915-921.
- Wollrab, E., Kulkarni, S. M., Ouyang, C. and Shah, S. P. (1996), "Response of reinforced concrete panels under uniaxial tension", *ACI Struct. J.*, **93**(6), 648-657.